Journal of Hazardous Materials 480 (2024) 136326

Contents lists available at ScienceDirect

Journal of Hazardous Materials

journal homepage: www.elsevier.com/locate/jhazmat

Mechanisms underlying Th2-dominant pneumonia caused by plastic pollution derivatives (PPD): A molecular toxicology investigation that encompasses gut microbiomics and lung metabolomics

Surui Lu [a,1], Qing Feng [a,1], Mingqing Chen [b], Xin Zeng [a], Huaqin Wei [a], Qizi Chen [a], Hai Guo [c], Liqin Su [d], Biao Yan [a,e], Yang Wu [a,e], Xu Yang [a,e,f], Ping Ma [a,e,*]

[a] Key Laboratory of Environmental Related Diseases and One Health, Xianning Medical College, Hubei University of Science and Technology, Xianning 437100, China
[b] Section of Environmental Biomedicine, Hubei Key Laboratory of Genetic Regulation and Integrative Biology, College of Life Sciences, Central China Normal University, Wuhan 430079, China
[c] Department of Civil and Environmental Engineering, The Hong Kong Polytechnic University, 999077, Hong Kong
[d] National Institute of Environmental Health, Chinese Center for Disease Control and Prevention, Beijing 100050, China
[e] Hubei Industrial Technology Research Institute of Intelligent Health, Xianning 437100, China
[f] Institute of Eastern-Himalaya Biodiversity Research, Dali University, Dali 671003, Yunnan, China

HIGHLIGHTS

- A new concept of plastic derivatives was proposed, and a model for PPD was created in this study.
- PPD-induced pneumonia involved in both chemical and Th2-predominant pneumonia.
- Lung cell ferroptosis and NFκB pathway mediated the ROS induced Th2-predominant pneumonia.
- PPD can induce the occurrence of pneumonia by altering the gut microbiota composition.

GRAPHICAL ABSTRACT

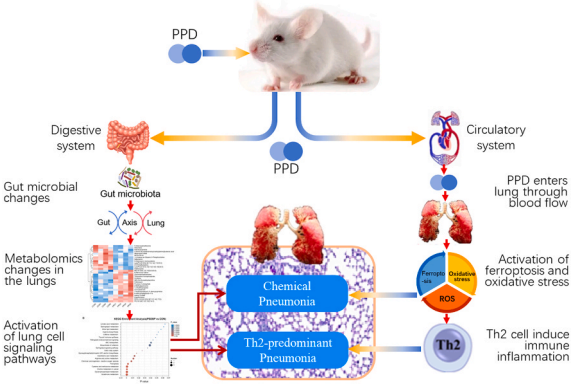

ARTICLE INFO

Keywords:
Plastic pollution derivatives (PPD)

ABSTRACT

An investigation was conducted by researchers on how dibutyl phthalate (DBP) and polystyrene microplastics (PS-MP) influence the development of pneumonia using a mouse model. For a duration of five weeks, the mice

Abbreviations: DBP, dibutyl phthalate; H&E, hematoxylin and eosin staining; LSD, least significant difference; MT, Masson trichrome staining; OPLS-DA, orthogonal least partial squares discriminant analysis; PAS, periodic acid-schiff staining; PE, polyethylene; PLA, polylactic acid; PS, polystyrene; PVC, polyvinyl chloride; RSD, relative standard deviation; TNF-α, tumor necrosis factor-α; DFO, deferoxamine; LEfSe, Linear discriminant analysis Effect Size; MCH, acetylcholine; OTUs, operational taxonomic units; PAEs, phthalates or phthalate esters; PCoA, principal co-ordinates analysis; PET, polyethylene terephthalate; PPD, plastic pollution derivatives; PS-MP, polystyrene microplastics; ROS, reactive oxygen species; SCFA, short chain fatty acid; VIP, Variable importance in the projection.

* Correspondence to: Hubei University of Science and Technology, No. 88 Xianning avenue, Xianning 437100, China.
E-mail addresses: maping@hbstu.edu.cn, mping68@126.com (P. Ma).

[1] Co-first authors. These authors contributed equally to this work.

https://doi.org/10.1016/j.jhazmat.2024.136326
Received 14 September 2024; Received in revised form 25 October 2024; Accepted 25 October 2024
Available online 26 October 2024

Th2-predominant pneumonia
Gut microbiome
Metabolomics
Short chain fatty acid (SCFA)

were subjected to exposure of DBP (30 mg/kg/day) and PS-MP (0.1 mg/day). The findings indicated notable pathological alterations in airway tissues, increased oxidative stress levels, and intensified inflammation, thereby establishing a connection between plastic pollution and pneumonia. Further examination indicated the involvement of ferroptosis and oxidative stress in the progression of the disease. Administration of deferoxamine (DFO) (100 mg/kg) resulted in symptom relief and reduced pathological alterations, as validated by metabolomic investigations. Increased levels of reactive oxygen species (ROS) triggered a Th2-mediated eosinophilic inflammatory response, marked by elevated IL-4 and reduced IFN-γ via the NFκB pathway. Moreover, analyses of the gut microbiome and metabolomics demonstrated that PPD modifies microbial populations and pulmonary metabolism, linking its effects on pneumonia through the gut-lung axis. This research highlights the health hazards associated with plastic pollution and proposes a framework for tackling these issues.

1. Introduction

The current situation of plastic pollution: Plastic products are integral to daily life, with global production nearing 400 million tons annually. However, only 9 % of plastic waste is recycled, 12 % incinerated, and the remainder ends up in landfills or the environment. This inefficiency has led to severe pollution issues: 9 to 23 million tons of plastic waste enter aquatic systems each year, and land-based plastic waste was estimated at 13 to 25 million tons in 2016, potentially doubling by 2025. Current disposal methods, such as landfilling, marine dumping, and open burning, cause soil, marine, and air pollution, disrupting agriculture and ecosystems. Furthermore, microplastics generated from the degradation of plastics can infiltrate the food chain, posing risks to both environmental and human health. Kibria et al. [1,2].

Microplastics (PS-MPs): Plastics degrade into microplastics (MPs) through complex physical, chemical, and biological processes when exposed to the environment [3]. Since their recognition, microplastics have become a major global research focus due to their environmental impact [4]. About 92 % of global plastic waste consists of microplastics, which range from 1 μm to 5 mm in diameter [5]. Key types include polystyrene (PS), polylactic acid (PLA), polypropylene (PP), polyvinyl chloride (PVC), polyethylene terephthalate (PET) and polyethylene (PE). Their small size and chemical stability mean they are widespread in the environment [6]. Marine species, from plankton to large mammals, ingest microplastics, which are found in 83 % of animal gastrointestinal tracts. Microplastics have also been detected in fruits and vegetables, suggesting plant absorption from soil [7]. They enter the food chain, posing health risks and making plastic pollution a pressing environmental issue [6]. Ingested microplastics can cause physical harm, physiological changes, and affect feeding, growth, reproduction, and oxygen consumption [2]. Microplastics, released throughout the lifecycle of plastic products, can enter human body through ingestion, skin contact, or inhalation, accumulating in organs. The World Wide Fund for Nature estimates that humans may consume up to 5 g of microplastics weekly. Recent studies have found microplastics in human blood, breast milk, placenta, and respiratory tract, linking them to respiratory issues, endocrine disruption, inflammatory bowel disease, and cancers [8].

Dibutyl phthalate (DBP): Dibutyl phthalate (DBP) is a common plasticizer used in cosmetics, food packaging, medical devices, construction materials, and electronics. It can leach into the environment throughout the lifecycle of plastics, accumulating in organisms and posing risks to both terrestrial and aquatic life. DBP is a significant endocrine disruptor and is frequently found in rivers and oceans due to its tendency to leach from microplastics [3]. Plasticizers like DBP enhance plastic flexibility and are consumed globally at about 7.5 million tons annually [4]. Phthalic acid esters (PAEs), including DBP, are present in air, water, soil, indoor dust, and food [9]. With a global production of approximately 5.5 billion tons, DBP is found in various environmental matrices in concentrations from nanograms to micrograms [10]. Its weak bonds with plastics facilitate its environmental release [11]. DBP exposure is linked to endocrine disruption, immune modulation, and inflammation, though its lung toxicity effects are less understood [12,13].

As plastics degrade into microplastics, they release DBP and other chemicals due to their increased surface area [2]. Microplastics, being small, hydrophobic, and with a large surface area, interact with other pollutants, potentially enhancing their combined toxicity [14]. Therefore, microplastics may amplify DBP's toxic effects through synergistic interactions.

Plastic pollutants ingestion and their toxic effects: Humans are primarily exposed to plastic pollutants through inhalation and ingestion. Inhalation occurs via contaminated air, such as particulate matter or industrial emissions, while ingestion happens through bottled water, packaged foods, or produce from polluted areas [15]. Ingested microplastics can adversely affect growth, development, and physiological health, potentially leading to mortality. They also absorb pollutants, impacting human health through the food chain by affecting genes, brain development, and respiratory function [16]. Microplastics have low absorption rates in the gastrointestinal tract, usually less than 1 %, despite some particles smaller than 150 micrometers penetrating the intestinal barrier. In aquatic organisms, microplastics can cause oxidative stress, cellular toxicity, and intestinal blockage. Studies in mammals like mice show that high doses of microplastics can lead to oxidative stress, inflammation, particle translocation to organs, and disruption of microbial communities [17]. However, research is still insufficient to fully understand the toxicity and mechanisms of orally ingested microplastics.

Association of plastic pollution with pulmonary inflammation: Lung tissue is essential for gas exchange and is particularly susceptible to exposure to PS-MPs and DBP. While direct evidence linking PS-MPs to human lung diseases is limited, studies using cellular and animal models reveal their potential effects. Laboratory experiments show that PS-MPs can alter cell structure, impede growth, and increase reactive oxygen species (ROS) production in human lung cells. Research on rats and mice indicates that PS-MPs cause lung damage, inflammation, and fibrosis [6]. The study by Han et al. [18] indicated that after gavage exposure to PS-MPs, pathological changes occurred in the lungs tissues of mice. The large surface area of PS-MPs enhances their ability to absorb and generate ROS, disrupting oxidative balance [19]. Li et al. [20] found that gavaging PBD ultimately led to pathological changes in the lung tissue of mice too.

Combined analysis of gut microbiota and metabolomics in the study of pollutant mechanisms: The gut microbiota is essential for immune regulation and intestinal health, encompassing both microbial communities and their genetic information [21]. Metabolomics analyzes metabolites to understand their roles in physiological and pathological changes [22], with untargeted metabolomics focusing on discovering metabolite changes due to biological system manipulations [23]. The gut microbiota affects not only local intestinal health but also distant tissues like the liver and brain through its metabolites [24,25]. Changes in microbial structure and metabolism can drive disease development [26]. Combining gut microbiota analysis with metabolomics helps explore pollutant toxicity mechanisms. For instance, reduced gut microbiota diversity can contribute to allergic airway diseases, while D-tryptophan supplementation may repair metabolic damage [27-29]. Research shows that pollutants like PM2.5 and PS-MPs can disrupt gut microbiota and increase harmful bacteria [15,30]. DBP exposure alters

gut microbiota composition, boosting pathogenic bacteria and reducing beneficial ones [31]. However, the precise mechanisms of microplastics' toxic effects remain unclear, though metabolic changes linked to dysbiosis are known risk factors for various adverse outcomes [32].

Previous research has linked particulate matter (PM) exposure to lung diseases and mouse models of lung injury [33]. In our previous research, we found that plastic pollution derivatives (PPD) formed by the combination of PS-MPs and DBP significantly exacerbate asthma in mice [34]. Additionally, monitoring respiratory system indicators in mice exposed to PPD suggested that PPD may pose a risk of inducing pneumonia. Therefore, this study conducted a detailed investigation into the relationship between PPD exposure and the occurrence of pneumonia, as well as the underlying mechanisms involved. Pathological assessments, including H&E, Masson's trichrome, and PAS staining, revealed inflammation and histological changes in lung tissues. Key indicators such as lung organ coefficients, oxidative stress, and inflammation were measured to understand PPD's toxicity. Integrating gut microbiota and lung tissue metabolomics, the study identified molecular mechanisms by which PPD induces lung inflammation through oxidative stress and ferroptosis along the gut-lung axis. Additionally, the study demonstrated that deferoxamine (DFO), an iron chelator and ferroptosis inhibitor, alleviated eosinophilic pneumonia induced by PPD.

The scientific hypothesis of the study: Drawing on earlier studies alongside our present results, we propose that contact with derivatives of plastic pollution (PPD) may lead to pneumonia (Fig. 1). The primary molecular mechanism involves PPD small molecules entering the bloodstream via the gut, inducing ferroptosis in lung tissue cells through systemic circulation. This leads to oxidative stress and establishes a feedback loop between these pathways, resulting in heightened ROS levels in lung tissue mediated by the NFκB pathway. This, in turn, triggers Th2-predominant pneumonia characterized by elevated levels of IL-4, IL-5, and eosinophils in the lung, alongside decreased INF-γ levels. IL-4 facilitates the differentiation of B cells into plasma cells that produce IgE. Furthermore, alterations in the gut microbiome structure play a role, leading to changes in the metabolic profile such as reduced synthesis of short-chain fatty acids (SCFA), increased synthesis of glycerophospholipids, and disruptions in various amino acid synthesis pathways. These modifications further exacerbate the aforementioned processes via the gut-lung axis, ultimately contributing to the development of pneumonia.

2. Materials and methods

2.1. Experimental animals

Sixty SPF-grade male Balb/C mice (20 ± 2 g), aged 4–5 weeks, were sourced from Hunan Slake Jinda Laboratory Animal Co., Ltd. Following a one-week acclimation in a pathogen-free environment, they were kept at 22–25 °C and 50–70 % humidity with ad libitum access to food and water. The study received ethical approval from the Ethics Committee of Hubei University of Science and Technology, with the approval certificate ID: HBUST-IACUC-2021–010 available upon request.

2.2. Reagents and kits

DBP (>99 %, CAS: 84–74-2), deferoxamine (DFO, CAS: 70-51-9), and mechlorethamine (MCH, CAS: 50-86-7) were all from Sigma-Aldrich. PS-MP particles (size: 5.125 ± 0.126 μm, more detail characterization of the PS-MP please see Fig. S1) were from Tianjin BaseLine ChromTech Research Centre. Tween-80 (CAS: 9005–65-6) was from Amresco (Solon, OH, USA). IL-4, IL-1β, T-IgE, TNF-α, IFN-γ, and recombinant Glutathione Peroxidase 4 (GPx4) were measured using ELISA kits from Shanghai Enzyme-linked Biotechnology Co. (Shanghai, China). Assay kits for ROS, GSH, and iron ions specific to mice were provided by Nanjing Jianjian Bioengineering Institute (Nanjing, China).

2.3. Experimental protocol

Human exposure to microplastics has been estimated using current mathematical models: the exposure dose we used was 0.1 mg/d, based on the references provided below. Research indicates that, on average, humans ingest about 10^7 microplastic particles annually [35], which is equivalent to approximately 2.7×10^4 particles per day. However, certain individuals, such as tea drinkers, may ingest significantly higher amounts of microplastics. For instance, brewing a plastic teabag at the

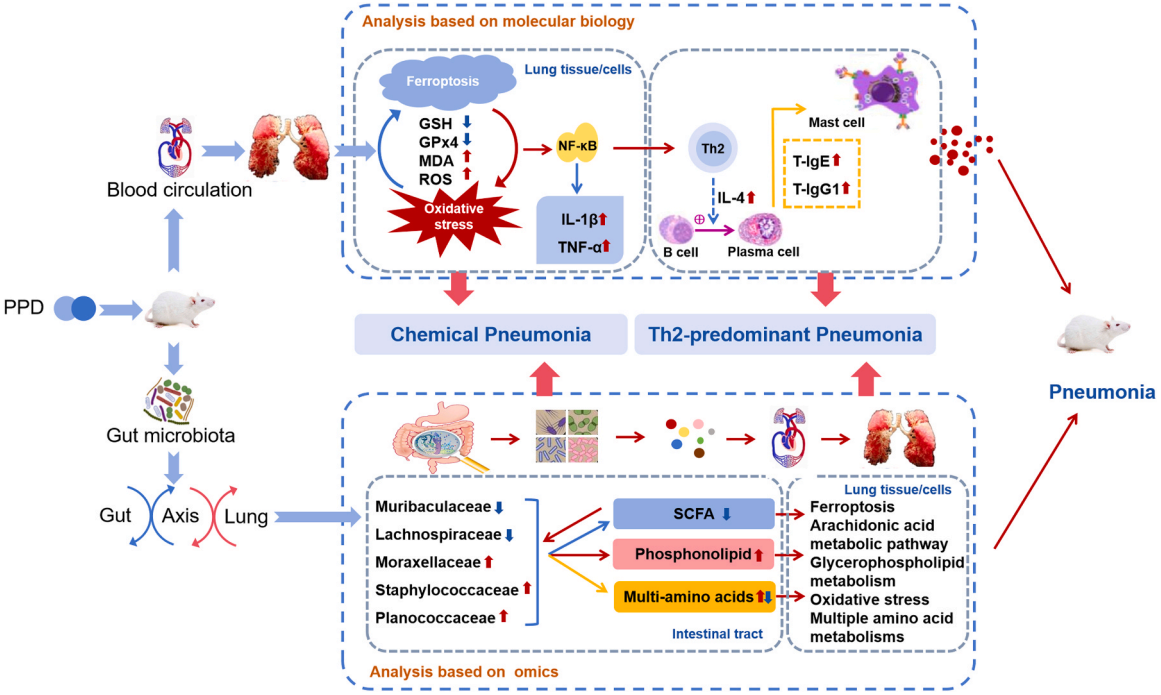

Fig. 1. Scientific hypothesis of the study.

appropriate temperature can release about 1.16×10^{10} microplastic particles into a cup of tea [36]. In this study, an intermediate concentration was estimated, with a purchased microplastics concentration of 10 mg/mL and a content of 1.4×10^{8} particles/mL. Mice were given a dose of 0.1 mg/d, which corresponds to 1.4×10^{6} particles, representing an intermediate concentration between the two references. Following a 5-week oral administration of DBP (30 mg/kg/d), mice exhibited leukopenia for 1 week, while adults exposed to DBP experienced a sustained immune suppressive effect, indicating increased susceptibility to disease [37].

Sixty male Balb/c mice were randomly divided into three experimental groups: (1) CON, (2) CON+PPD, and (3) CON+PPD+DFO (Table 1). The PPD group was administered 30 mg/kg/day DBP and 0.1 mg/day PS-MP, with DBP dissolved in normal saline containing Tween-80. DFO was given intraperitoneally at a dose of 100 mg/kg every two days [38]. Each group included 20 mice, allocated as follows: 6 for lung function assessments, 6 for molecular pathology (biomarker analysis in the left lung homogenate and pathological examination of the right lung), 4 for gut microbiome and lung metabolomics studies, 2 for electron microscopy, and 2 as reserves (Fig. 2). To obtain valid data, the personnel responsible for the experimental grouping operations were not the same as the researchers involved in the measurement of experimental data.

2.4. Serum and tissue sample preparation

On day 37 of the experiment, mice were euthanized, and blood and lung tissue were collected and processed [34].

2.5. Lung histological assay

Prepare sections from the pre-processed lung tissue samples, and stain them using hematoxylin and eosin (H&E), periodic acid-Schiff (PAS), and Masson's trichrome (MT) methods. The stained sections were subsequently examined under a Nikon Eclipse 80i microscope [34].

2.6. ELISA assay

An Enzyme-Linked Immunosorbent Assay (ELISA) assessed immune and inflammatory markers in serum and lung tissue. T-IgE was used to detect Type I hypersensitivity, while IL-4 and IFN-γ measured Th1/Th2 balance. IL-1β and TNF-α evaluated inflammation due to oxidative stress. Additionally, ROS, MDA, GSH, GPx4, and ferric ions were examined to study oxidative stress and ferroptosis. All tests followed the reagent guidelines precisely.

2.7. Mitochondrial electron microscope

Prepare fresh lung tissue into sections according to standard procedures [34]. The sections were then analyzed using a transmission electron microscope (HT7800/HT7700, HITACHI, Japan).

Table 1
Grouping and group treatments.

Group ID	Group names	Treatments for different groups			
		Saline (Contral)	Gavage 30 DBP	Gavage 0.1 PS-MP	DFO I.P. injection
Group 1	Control (CON)	+	–	–	–
Group 2	CON+PPD	+	+	+	–
Group 3	CON+PPD+DFO	+	+	+	+

2.8. Microbiomics analysis of feaces

Mouse feces were collected. The genomic DNA of total microbial was extracted. The specific methods can be found in the supporting information.

2.9. Untargeted metabolomics analysis of lung tissue

Process tissue samples according to standard methods and analyze them using LC-MS. The specific data analysis methods can be found in the supporting information.

2.10. Statistical analysis

Data were collected in six replicates and presented as mean ± standard deviation. Statistical analysis was performed using SPSS 26.0, and data visualization was conducted with GraphPad Prism 9.0. One-way ANOVA combined with the least significant difference (LSD) method was utilized to assess statistical significance, with a threshold of $P < 0.05$. For metabolomics, metabolites were deemed significantly different if they had a VIP > 1 and $P < 0.05$, based on the OPLS-DA model and Student's t-test. Similarly, gut microbiome data were analyzed using one-way ANOVA and LSD, maintaining the statistical significance threshold at $P < 0.05$.

3. Results

3.1. The pathological changes in lung following PPD exposure

Compared to the CON group, the CON+PPD group of mice exhibited a noteworthy increase in lung tissue organ coefficient (Fig. 3A). The airways displayed dilation and distortion of folds, characterized by inwardly forming folds and thickened airway walls. Extensive deposition of blue-stained collagen around lung tissue airways was evident both internally and externally, accompanied by an elevated number of bronchial goblet cells. Additionally, there was a noticeable accumulation of mucus inside and outside the airways, leading to altered airway morphology (Fig. 3B). These observations indicate significant airway remodeling in the CON+PPD group. From a pathological perspective, the CON+PPD+DFO group showed improvement compared to the CON+PPD group, with a significant trend toward normalization to the CON group (Fig. 3B and B).

3.2. Changes of the related factors in oxidative stress and ferroptosis in lung following PPD exposure

The Fig. 4 displays the results of evaluating biochemical markers associated with ferroptosis and oxidative stress levels. Mice in the CON+PPD group showed notably higher levels of the ferroptosis-related biochemical marker Fe^{2+}, as well as increased levels of ROS and MDA compared to the CON group. In contrast, levels of GSH and GPx4 were significantly reduced. Treatment with DFO resulted in a shift of these markers towards levels similar to those in the Saline group as opposed to the PPD group, with statistical significance.

3.3. Morphological changes of mitochondria

Mitochondrial morphology plays a critical role in the assessment of ferroptosis. To investigate this, we utilized electron microscopy to examine mitochondria in cells. In the CON+PPD group, mitochondria appeared sparse and disorganized, exhibiting significant damage including fragmented and blurred cristae, with some mitochondria resembling vacuoles. These findings indicate that ferroptosis may have occurred in the lung cells of the mice. Following treatment with DFO, the extent of mitochondrial damage was reduced, though some vacuoles remained present. Furthermore, there was a partial normalization of

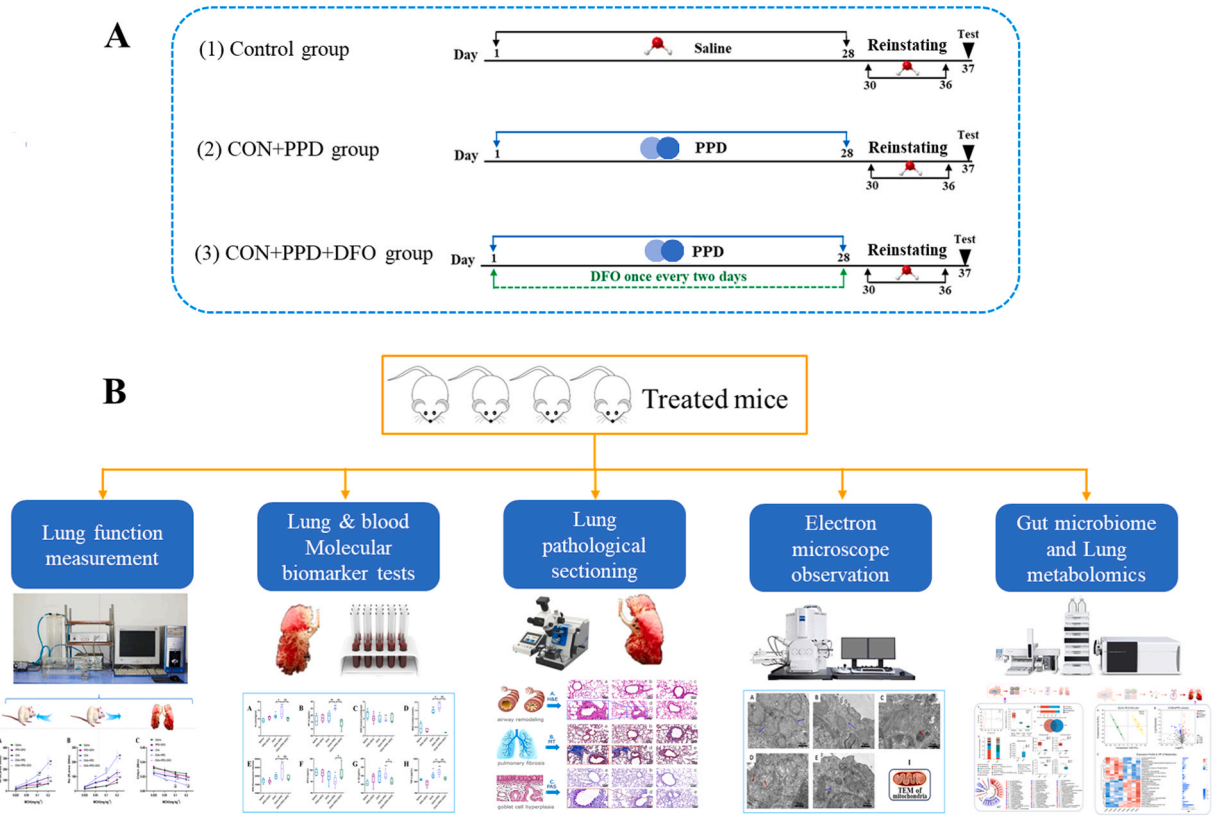

Fig. 2. Experimental protocol. (A) Grouping and experimental schedule; (B) The analytical techniques used in this study.

mitochondrial cristae morphology, characterized by clear double membranes and an abundance of normal mitochondria (Fig. 5).

3.4. Indicator of chemical pneumonia

The Fig. 6 illustrates two key indicators of chemical pneumonia caused by PPD exposure in mice. In comparison to the CON group, the levels of IL-1β and TNF-α were notably higher in the CON+PPD group. However, after treatment with DFO, there was a significant decrease in the levels of IL-1β and TNF-α.

3.5. Indicator of Th2-predominant pneumonia

In this study, we examined the impact of PPD exposure on pneumonia development by measuring Th1-type cytokine IFN-γ and Th2-type cytokine IL-4 (Fig. 7). The CON+PPD group exhibited a significant increase in IL-4 levels and a decrease in IFN-γ levels compared to the CON group. Additionally, the IL-4/IFN-γ ratio was significantly reduced, serum T-IgE were also evaluated. Fig. 7 shows a notable increase in the CON+PPD group compared to the CON group. Importantly, treatment with the antagonist DFO effectively suppressed these effects.

3.6. The impact of PPD exposure on the gut microbiota in mice

Research increasingly indicates that external stimuli can disrupt the gut microbiota, potentially worsening lung damage through the gut-lung axis. To explore the effects of PPD exposure on gut microbiota, fecal samples from PPD-exposed mice were sequenced using 16S rRNA amplicons. This study assessed alpha diversity, which measures sample richness and evenness. To identify differences in gut microbiota between the CON+PPD and CON groups, beta diversity was analyzed. Principal Coordinates Analysis (PCoA) was utilized to visualize and compare variations between and within groups (Fig. 8A). To examine the impact of PPD exposure on microbial composition and structure, samples were analyzed at the family level. Fig. 8C shows that 55 microbial taxa were identified in the CON group. A total of 54 microorganisms were detected in the CON+PPD group, with 45 microorganisms present in both groups of samples. The gut microbiota of the mice primarily consists of *Muribaculaceae* and *Lactobacillaceae* (Fig. 8D). In comparison to the CON group, the CON+PPD group exhibited the decrease in the *Muribaculaceae, Lachnospiraceae, Bacteroidaceae* and an increase in the *Lactobacillaceae* (Fig. 8D). And multiple flora such as *Staphylococcaceae, Planococcaceae* and *Rikenellaceae* are appeared (Fig. 8D). The analysis indicated notable differences in the gut microbiota structure across the various mouse groups. To further identify the differential bacterial species in each group, Linear Discriminant Analysis Effect Size (LEfSe) was performed (Fig. 8E). LEfSe was applied to microbial taxa ranging from phylum to genus level, with a threshold of LDA score > 2 and $P < 0.05$. Among the identified differentially abundant species, 78 were found to be enriched in the CON group, including *Muribaculaceae, Lachnospiraceae, Erysipelatoclostridiaceae* which are belong to firmicutes, as well as 51 dominant species in the CON+PPD group, such as *Staphylococcaceae, Bacillus, Planococcaceae*.

3.7. Changes in pulmonary tissue metabolomics

To better understand the effects of PPD ingestion on lung tissue in mice, we performed metabolomic analyses to explore metabolic changes within the lung tissue. As shown in Fig. 9A, Partial Least Squares Discriminant Analysis (PLSDA) revealed distinct differences in metabolite profiles between the CON and CON+PPD groups following PPD exposure. These differences were further highlighted by the volcano plot (Fig. 9B). To identify potential biomarkers for differentiating between the groups, we applied a VIP threshold of > 1. The top 30 metabolites that met this criterion were then visualized in a heatmap (Fig. 9C). Significant differences in metabolites included S-Adenosylmethionine,

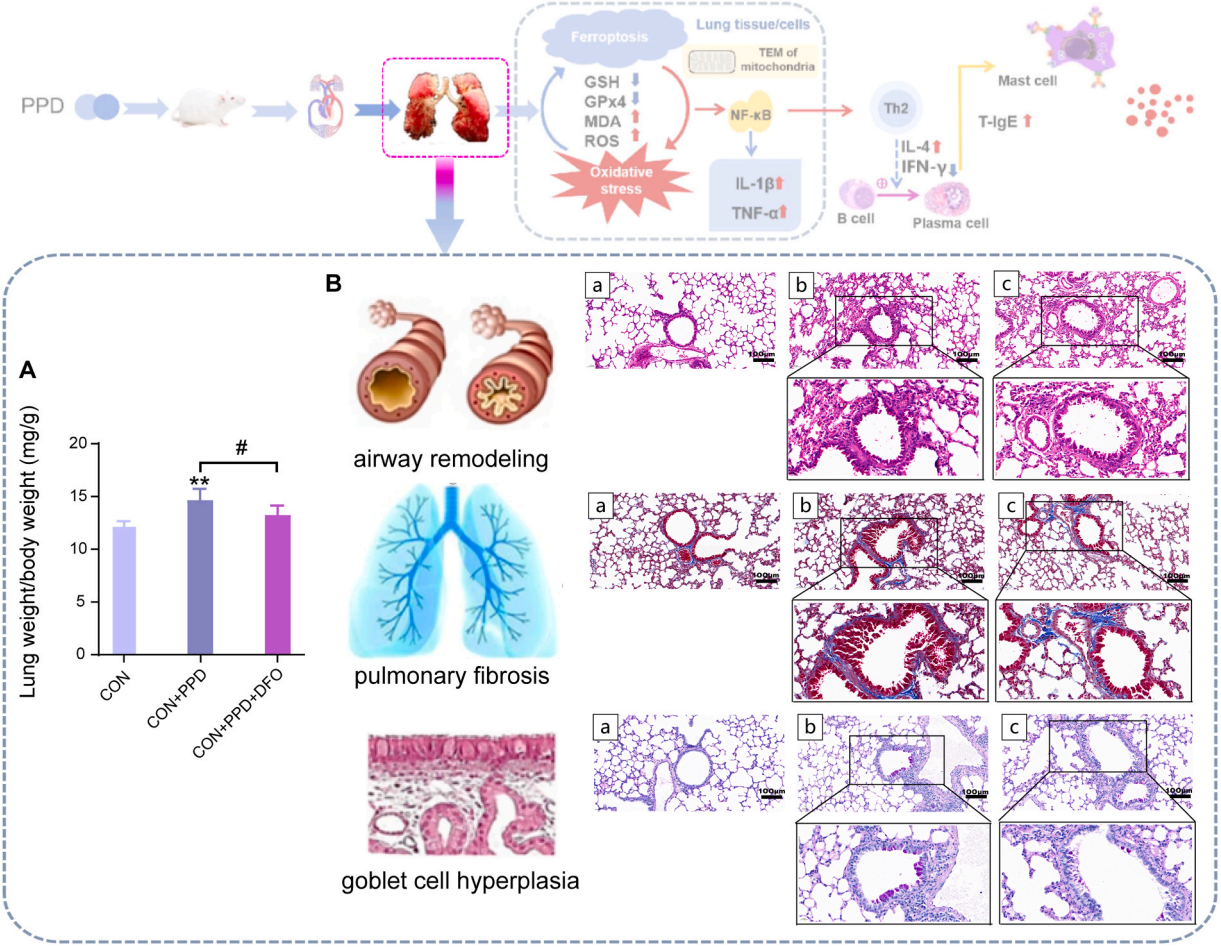

Fig. 3. Histopathological staining of lung tissue. A. Organ coefficient. B. (1): Masson trichrome staining; (2): hematoxylin and eosin staining; (3): periodic acid-schiff staining. a: the CON group; b: the CON+PPD group; c: the CON+PPD + DFO group. ** : $p < 0.01$ compared with the Saline group. #: $p < 0.05$ compared with the PPD group.

salbutamol, ergothione and Ornithine, etc. The level of S-adenosylmethionine in CON+PPD group was significantly lower than the CON group. The content of salbutamol in the lung tissue sample of CON+PPD decreased significantly. It was worth noting that in the lung tissue samples of mice in CON+PPD group, the contents of ergothione and Ornithine were significantly increased.

In order to further explored the role of significantly different metabolites, we used KEGG Compound classification analysis to classify these different metabolites according to the biological roles in which the metabolites participated (Fig. 10A). Among them, lipid compounds were the most numerous, which corresponds to the conclusion that the differential microbial groups identified through microbiome data analysis lead to significant changes in short-chain fatty acid metabolism. After mapping these different metabolites to the KEGG pathway. It was found that these differential metabolites are indeed directly related to fatty acid metabolic pathways. And there also some different metabolites in amino acid metabolism and nucleotide metabolism. The goal of enrichment analysis is to pinpoint biological pathways that are crucial to a specific biological process, thereby enhancing our understanding of the underlying molecular mechanisms. Metabolites showing significant differences between groups (*t*-test, $p < 0.05$) were analyzed using KEGG-based methods to identify the metabolic pathways where these metabolites were significantly enriched (Fig. 10B). The enriched differential pathways include Arachidonic acid metabolism, Ferroptosis, Glycerophospholipid metabolism, ABC transporters, Pyrimidine metabolism, as well as amino acid metabolic pathways such as Glutathione metabolism, Cysteine and methionine metabolism, and Arginine biosynthesis.

3.8. Integrated analysis of microbiomics and metabolomics

Using the Spearman correlation method, we calculated the correlation coefficients between the top 100 dominant microbial groups and significant differential metabolites, and generated a correlation heatmap (Fig. S2). We identified several microbial groups, including *Lachnospiraceae*, *Muribaculaceae*, *Staphylococcaceae*, *Planococcaceae*, *Moraxellaceae*, *Erysipelatoclostridiaceae*, *Desulfovibrionaceae*, and *Rikenellaceae*, that were significantly associated with key differential metabolites. We conducted an in-depth correlation analysis using the Mantel test between these microbial groups and the key metabolites obtained from metabolomics analysis, finding that each microbial group was significantly associated with one or more key metabolites (Fig. 11A). Based on these correlation analysis results and the KEGG pathway enrichment results from metabolomics, we created a cascade relationship diagram illustrating the connections from microbes to metabolites to metabolic pathways (Fig. 11B). The primary microorganisms included *Bacteroidaceae, Moraxellaceae, Muribaculaceae, Lachnospiraceae, Rikenellaceae, Planococcaceae, Staphylococcaceae, Desulfovibrionaceae* and *Erysipelatoclostridiaceae*, and then linked to the metabolic substances including ergothioneine, glutathione oxidized, S-adenosylmethionine, 6-keto-prostaglandin fla, omithine, O-phosphoethanolamine, cystathionine, fructose 1-phosphate, etc. And associated with the pathways, Arachidonic acid metabolism, Ferroptosis, Chemical carciogenesis-reactive oxygen species, Sulfurrelay system, Glutathione metabolism, Cysteine

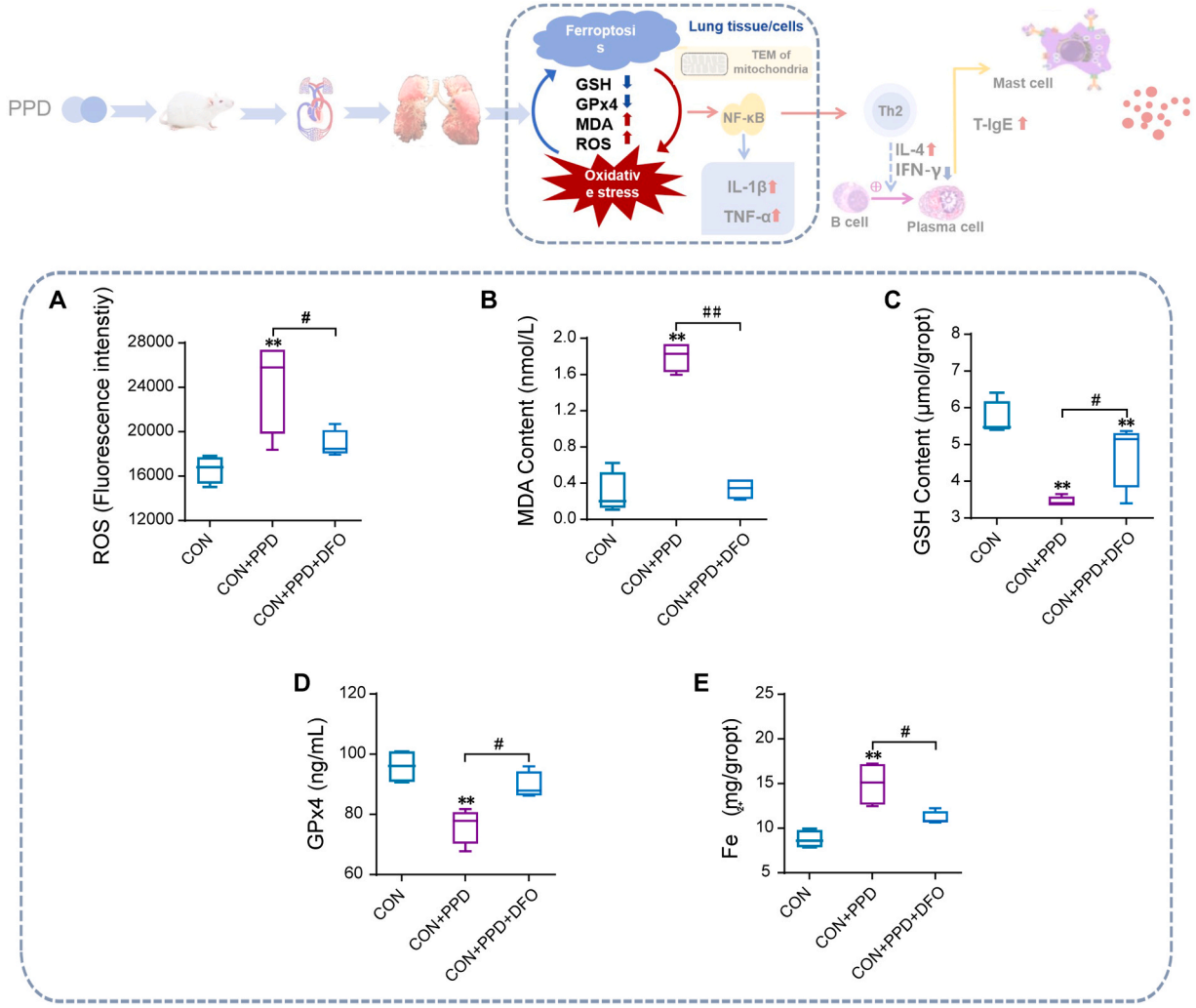

Fig. 4. Ferroptosis and oxidative stress indicators. (**: $p < 0.01$, compared with the CON group. #: $p < 0.05$, compared with the CON+PPD group. ##: $p < 0.01$, compared with the CON+PPD group.).

and methionine metabolism, Sphingolipid signaling pathway, Glycosylphosphatidylinositol anchorbiosythesis, Glycerophospholipid metabolism and Choline metabolism in cancer.

4. Discussion

4.1. Evidence that exposure to PPD induces pneumonia

The typical pathological changes observed in pneumonia include the infiltration of inflammatory cells in lung tissue, thickening of alveolar walls, lung tissue fibrosis, and narrowing of the airways due to edema [20]. This study highlighted significant pathological changes in lung tissue, such as infiltration of inflammatory cells and extracellular matrix deposition (Figure 3B1, H&E staining), airway remodeling characterized by thickening of the airway basement membrane (Figure 3B1, H&E staining), lung tissue fibrosis (Figure 3B2, MT staining), and hyperplasia of goblet cells (Figure 3B3, PAS staining). Moreover, the organ coefficient can effectively reflect the degree of organ damage [39]. The organ coefficient of the lung tissue in mice exposed to PPD was significantly elevated (Fig. 3A), indicating damage to the lung tissue. These findings provide strong evidence supporting the pivotal role of PPD in inducing pneumonia.

4.2. Activation of ferroptosis and oxidative stress induced by PPD as key drivers of pneumonia

After exposure to PPD, there was an increase in intracellular ROS, altered mitochondrial morphology, and iron overload. Treatment with DFO led to a significant reduction in ROS and Fe^{2+} levels, indicating the occurrence of ferroptosis (Fig. 4 and Fig. 5) [40]. Excessive ROS induced by PPD reacts with intracellular biomolecules, triggering immune responses and activating NF-κB, which promotes the expression of TNF-α and IL-1β, exacerbating lung tissue damage [41,42]. Our study showed that GSH and GPx4 levels were lower in the CON+PPD group of mice, while ROS, IL-1β, and TNF-α levels were higher compared to the CON group (Fig. 4 and Fig. 6), suggesting an imbalance in oxidative status in the lung tissue of PPD-induced pneumonia mice. The accumulation of excess free iron can worsen oxidative stress, leading to ferroptosis development [34,43]. Therefore, we propose that the combined effects of ferroptosis and oxidative stress are critical in the pathogenesis of pneumonia in mice.

4.3. PPD exposure increases the risk of Th2-predominant pneumoni in mice

Exposure to PPD (CON+PPD group) not only activated NF-κB in lung cells, leading to increased expression of TNF-α and IL-1β, but also notably elevated Th2 cell-mediated IL-4 levels compared to the CON

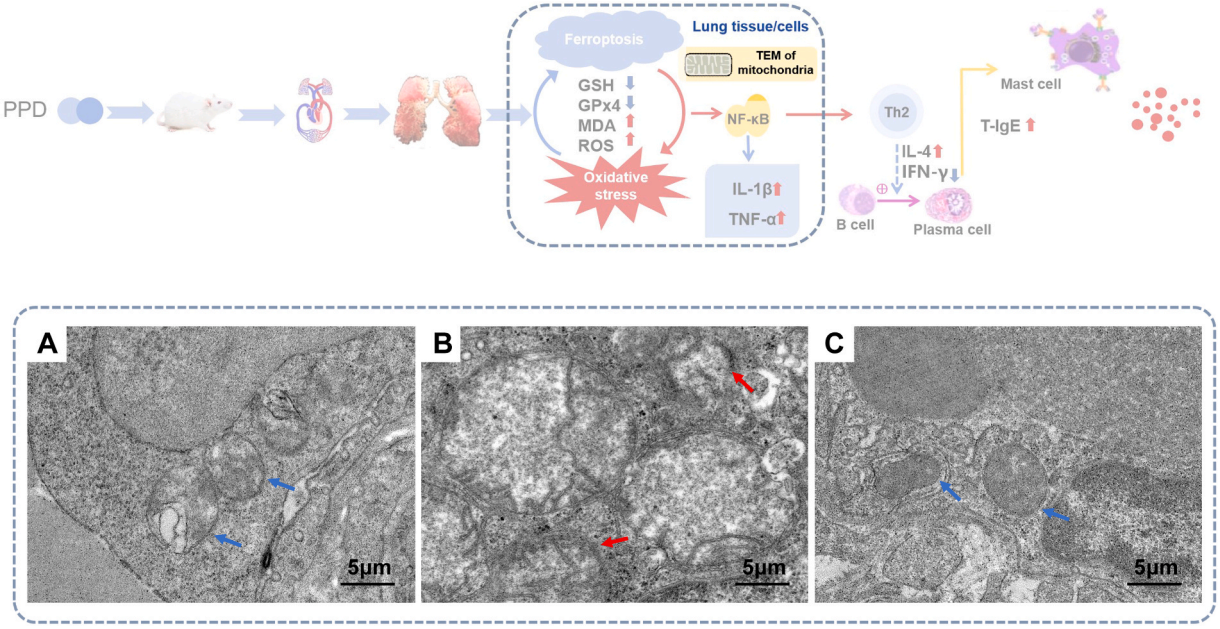

Fig. 5. Mitochondrial transmission electron micrographs of lung tissue cells. A: the CON group; B: the CON + PPD group; C: the CON + PPD + DFO group. The blue arrows show clear structure of mitochondrial cristae with intact membranes bilaterally; the red arrows show intramitochondrial vacuoles with broken membranes.

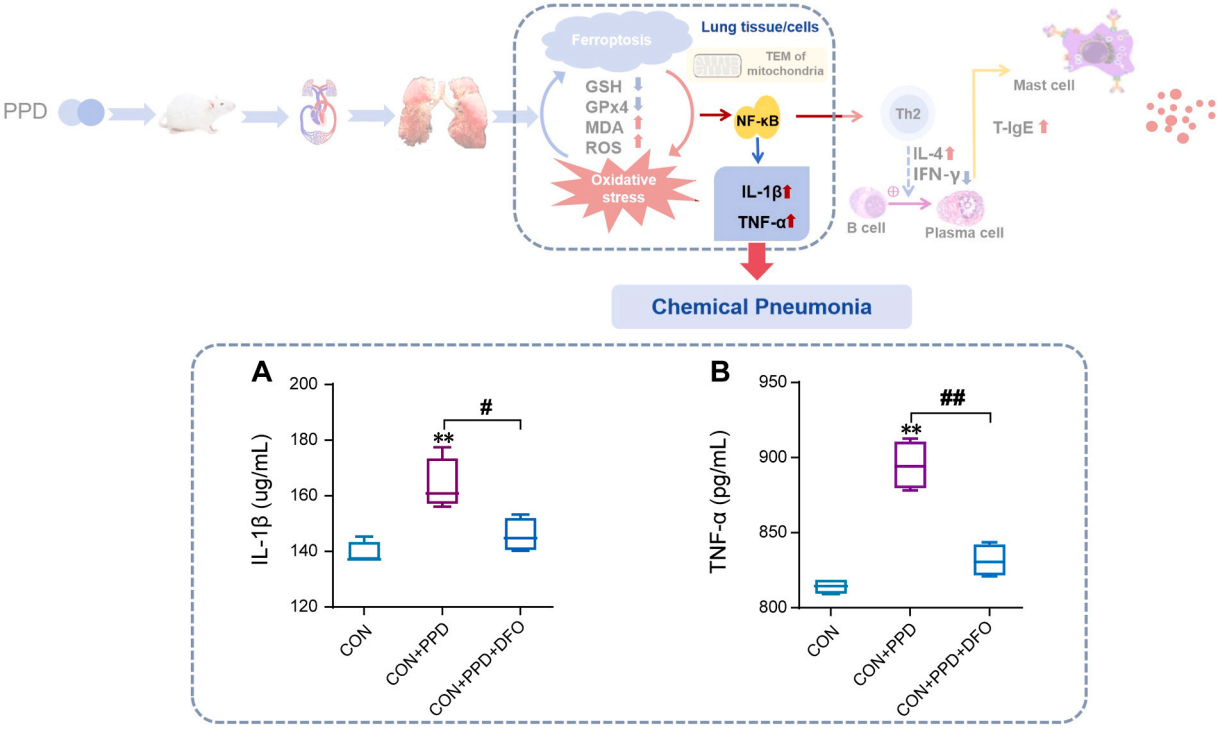

Fig. 6. Indicators of chemical pneumoni. (**: $p < 0.01$, compared with the CON group. #: $p < 0.05$, compared with the CON+PPD group. ##: $p < 0.01$, compared with the CON+PPD group.).

group, while decreasing IFN-γ levels (Fig. 6). Moreover, there was a significant increase in immunoglobulin T-IgE associated with type I hypersensitivity (Fig. 7). These findings indicate that increased ROS levels stimulate the differentiation and proliferation of Th0 cells into Th2 cells through the NF-κB signaling pathway [44]. The Th2 cells then produce higher amounts of IL-4 while reducing IFN-γ levels [45,46]. Elevated IL-4 levels promote the development of type I hypersensitivity reactions, which directly contribute to the onset and progression of allergic asthma [47,48]. This, in turn, enhances susceptibility to Th2-dominant pneumonia [49].

4.4. The impact of PPD exposure on the composition of gut microbiota in mice

In addition to being absorbed by the intestines and entering the lungs through systemic circulation to directly induce ferroptosis and oxidative stress, ultimately leading to pneumonia, PPD small molecules may also promote the occurrence of pneumonia by altering the gut microbiota

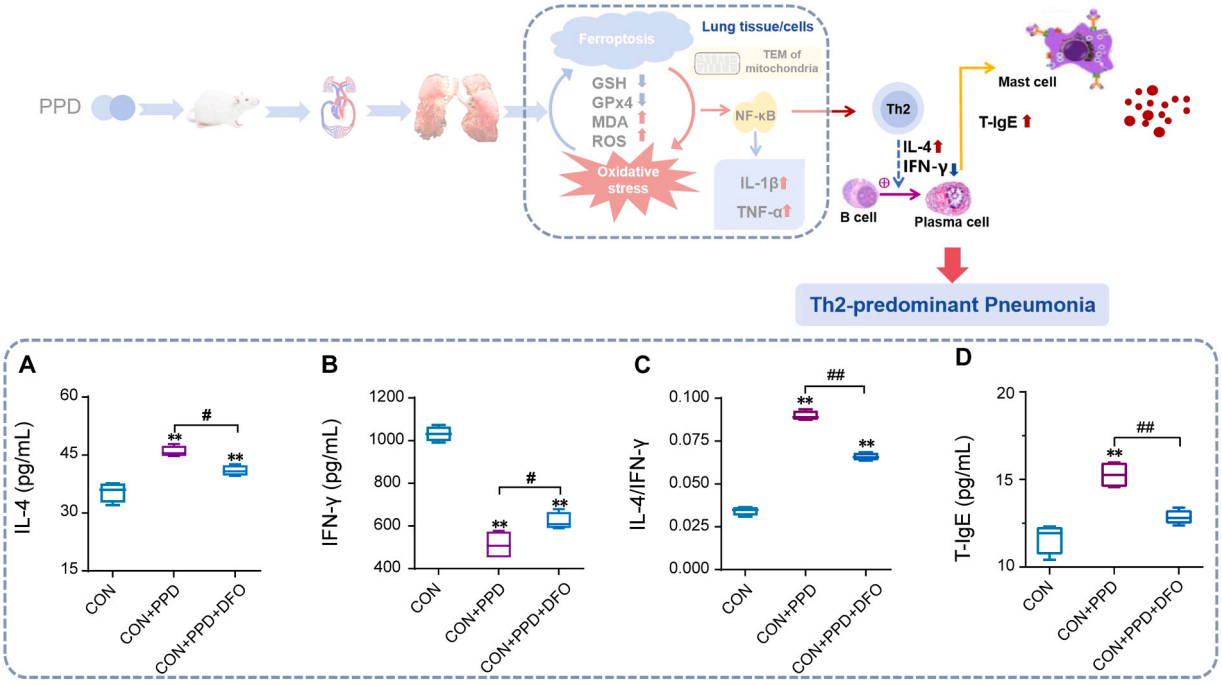

Fig. 7. Indicators of Th2-predominant pneumoni. (**: $p < 0.01$, compared with the CON group. #: $p < 0.05$, compared with the CON+PPD group. ##: $p < 0.01$, compared with the CON+PPD group.).

composition. The gut microbiota of mice in the CON and CON+PPD groups were distinctly different, indicating a significant change in the gut microbiota structure due to PPD exposure (Fig. 8B). In comparison to the CON group, the CON+PPD group exhibited the decrease in the *Muribaculaceae, Lachnospiraceae, Bacteroidaceae* and an increase in the *Lactobacillaceae* (Fig. 8D). Research shows that the *Bacteroidaceae* and *Lachnospiraceae* communities can metabolize fiber into short-chain fatty acids, and their increased abundance can effectively alleviate the development of emphysema [50]. Therefore, changes in the abundance of *Bacteroidaceae* and *Lachnospiraceae* are closely related to lung diseases. In this study, the significant decrease of *Bacteroidaceae* and *Lachnospiraceae* due to PPD exposure also reflects that PPD promotes the occurrence of lung diseases. And multiple flora such as *Staphylococcaceae, Planococcaceae* and *Rikenellaceae* are appeared (Fig. 8D). *Staphylococcaceae* are known to cause a range of infections in humans, beginning with skin and soft tissue infections and extending to more severe conditions such as endocarditis, sepsis, and pneumonia. This is also important evidence that PPD causes pneumonia by altering the composition of gut microbes. In Linear discriminant analysis Effect Size (LEfSe) analysis (Fig. 8E), there are some differentially abundant species. *Muribaculaceae, Lachnospiraceae, Erysipelatoclostridiaceae* were enriched in the CON group which are belong to firmicutes. Although the abundance of firmicutes in CON+PPD group increased significantly from the analysis of microbial composition of the two groups at the phylum level. The abundance of important producers of butyric acid and other sSCFAs [51], *Muribaculaceae* and *Lachnospiraceae,* has significantly decreased. Butyrate, a primary energy source for the intestinal mucosa, plays a crucial role in regulating bacterial energy metabolism, intestinal health, and host cell processes such as gene expression, inflammation, differentiation, and apoptosis [52]. The abundance of producers of butyrate in the gut microbiota significantly decreases during inflammation and rises after inflammation is suppressed [52]. Moreover, short-chain fatty acid (SCFA) signals, including butyrate, are vital for maintaining lung homeostasis and modulating intracellular defense mechanisms in alveolar cells. The reduction in short-chain fatty acid synthesis will decrease the defensive capacity of lung tissue [53]. Therefore, PPD may change SCFA synthesis by changing the composition of firmicutes in the intestinal tract of mice. Thus, causing intestinal flora imbalance and pulmonary inflammation through the entero-pulmonary axis. Changes in firmicutes do increase the risk of lung inflammation [54]. Meanwhile, dysregulation of gut microbiota is associated with mitochondrial damage in cells [55], thereby exacerbating cellular oxidative stress and inflammatory responses.

4.5. *The impact of PPD exposure on the metabolic profile of mouse lung tissue*

Significant differences in metabolites between group CON and group CON+PPD include S-Adenosylmethionine, salbutamol,ergothione and Ornithine, etc (Fig. 9C). S-adenosylmethionine is shown to be available through mediated epigenetic modification in IL-10-producing B cells to relieve pneumonia [28]. The level of S-adenosylmethionine in the CON+PPD group is significantly lower than that in the CON group, indicating that the inflammation risk in the CON+PPD group is higher than that in the CON group. Salbutamol is a short-acting β-2 adrenergic receptor agonist that can relax smooth muscle cells and inhibit cytokine release, making it effective for treating asthma and having anti-inflammatory effects [56]. The significant decrease of salbutamol in the CON+PPD group indicates a marked increase in the risk of respiratory diseases. It is worth noting that in the lung tissue samples of mice in CON+PPD group, the contents of ergothione and Ornithine were significantly increased. These two compounds are commonly found in lung cells damaged by external stimulation to alleviate the damage caused by such stimulation (Fig. 10A). This also indicates that the lung cells of the mice were indeed stimulated by PPD. Among the KEGG Compound classification analysis, lipid compounds were the most numerous, which corresponded to the conclusion of the microbiome data. It is found that these differential metabolites are indeed directly related to fatty acid metabolic pathways from mapping these different metabolites to the KEGG pathway. And there also some different metabolites in amino acid metabolism and nucleotide metabolism. Human amino acid metabolism is an essential component of nitrogen metabolism, directly associated with the synthesis of nitric oxide radicals, playing a significant driving role in the onset and progression of

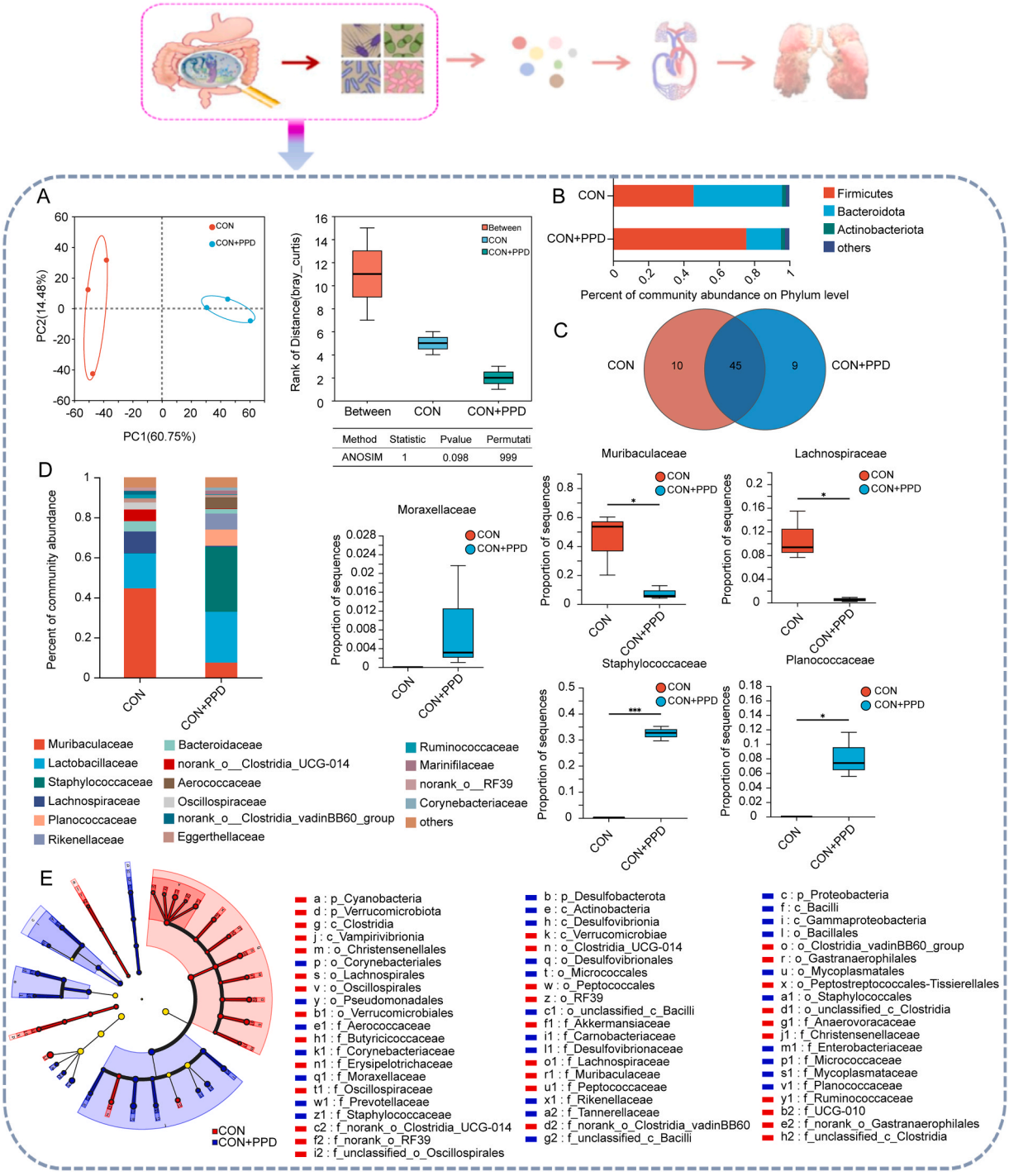

Fig. 8. Effects on mice gut induced by PPD exposure. A. β diversity. B. Alterations in microbiota at phylum level C. Venn diagram. D. Alterations in microbiota at genus level. E. LEfSe cladogram. *: $p < 0.05$, ***: $p < 0.001$.

pneumonia. Amino acid metabolism disorders can lead to decreased immune regulation and reduced protective capacity in the lungs. Zhang et al., [57]. KEGG enrichment analysis (Fig. 10B) suggest that Arachidonic acid metabolism is the differential pathways which is important target pathways that typically affect the alteration of intestinal microbiota in the synthesis of short-chain fatty acids [58]. In addition, amino acid metabolic pathways including Glutathione metabolism, Cysteine and methionine metabolism, Arginine biosynthesis were also enriched. ABC transporters, Pyrimidine metabolism, Glycerophospholipid metabolism,et al., they show significant differences, which is very similar to the changes in lung tissue metabolism caused by lung inflammation caused by PM2.5 [59]. It is worth noting that significant metabolic changes also occurred in ferroptosis, which is closely related to the development of pneumonia also [60]. This is also consistent with the significant increase in divalent iron content shown in Fig. 2E and the iron death characterized by mitochondrial damage in Fig. 5. That triggered our attention to various oxidation, inflammatory and immune indicators.

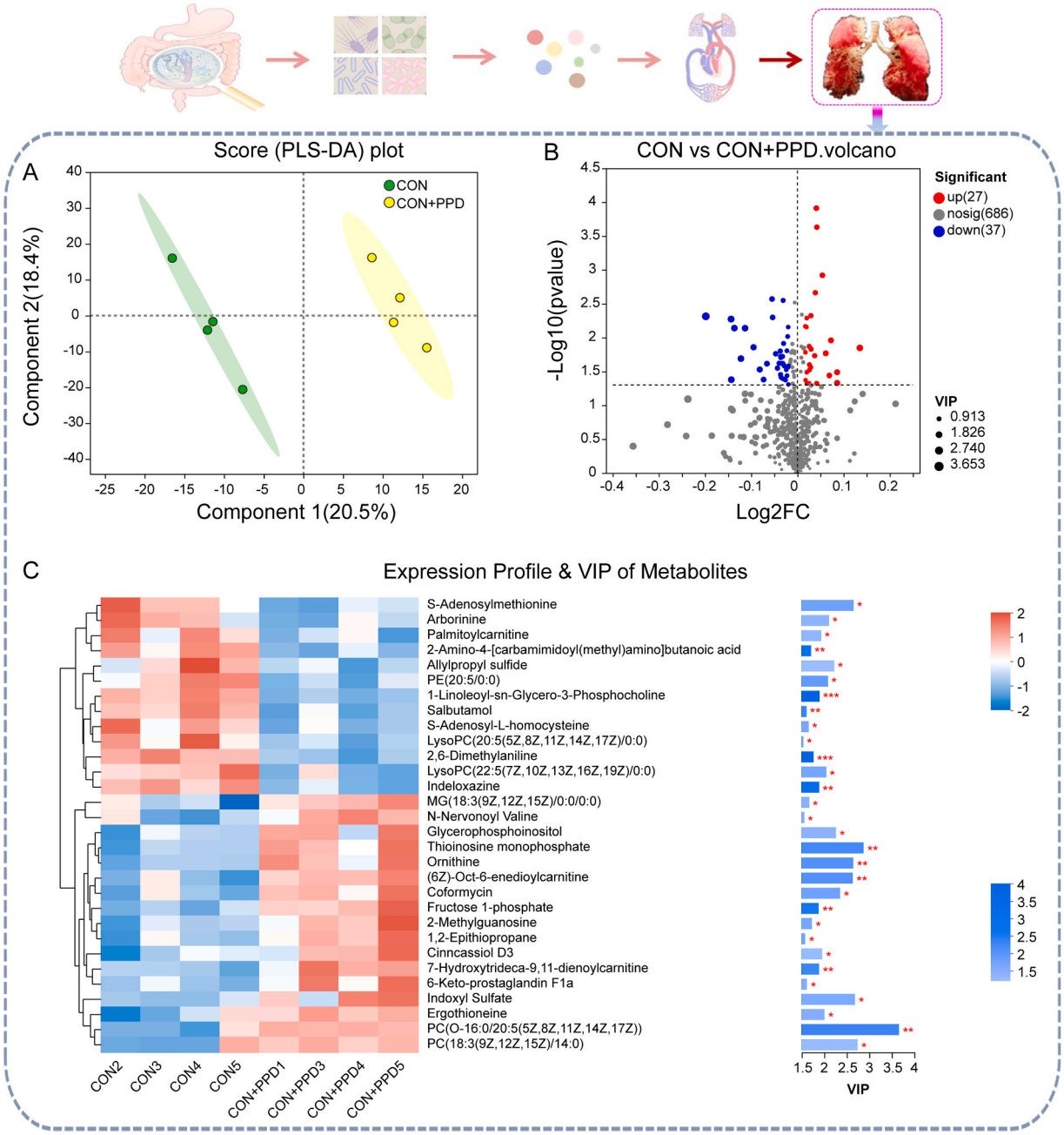

Fig. 9. Effects on metabolic profile of lung tissue induced by PPD exposure. A. PLS-DA score plot of CON and PPD groups. B. The differential metabolites between CON and PPD groups. C. Expression profile and VIP of metabolites. *: $p < 0.05$, **: $p < 0.01$, ***: $p < 0.001$.

4.6. Analysis of the association between gut microbiota and metabolic changes in lung tissue

Changes in the structure of the gut microbiota can lead to alterations in the intestinal metabolic profile. Through the gut-lung axis, these changes may further affect the metabolic profile of lung tissue. To analyze the connection between the microbiomics and metabolomics results, we first examined the correlation between dominant microbial communities and differential metabolites. This helps to identify microbial groups that are highly correlated with differential metabolites, which are likely key species influencing metabolic differences. Based on the number of significantly different metabolite factors and the magnitude of significant p-values, we ranked the top 100 microbial groups and created a heatmap (Fig. S2). In addition to the core gut bacteria *Lachnospiraceae*, *Muribaculaceae*, *Staphylococcaceae*, *Planococcaceae*, and *Moraxellaceae*, several other groups, including *Erysipelatoclostridiaceae* and *Desulfovibrionaceae*, also showed strong correlations with differential metabolites. Therefore, we conducted an in-depth correlation analysis using the Mantel-test to explore the relationships between these microbial groups and several key metabolites closely associated with the onset of pneumonia (Fig. 11A). The analysis results indicate that *Moraxellaceae*, *Muribaculaceae*, *Lachnospiraceae*, and *Staphylococcaceae* are significantly associated with the key metabolite 6-keto-prostaglandin F1α. *Muribaculaceae*, *Staphylococcaceae*, and *Planococcaceae* are significantly associated with O-phosphoethanolamine, ergothioneine, and ornithine, respectively. Additionally, *Desulfovibrionaceae* is not only significantly associated with ergothioneine but also closely related to fructose 1-phosphate and metabolites in the glycerophospholipid metabolism pathway. Ultimately, we illustrated this association through the cascade relationship of microbiota, metabolites, and metabolic

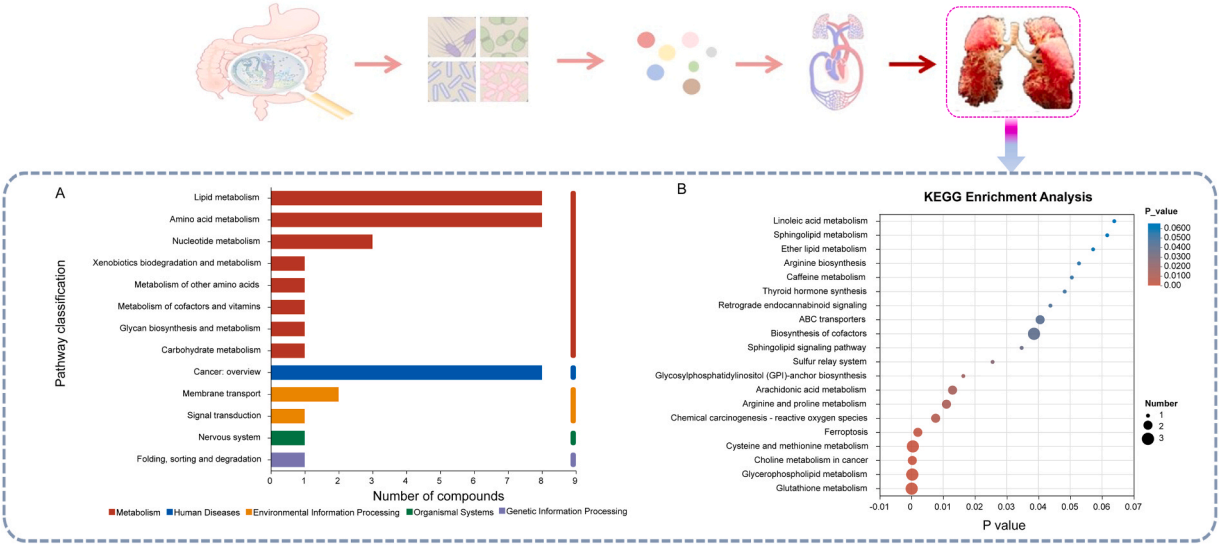

Fig. 10. Effects on metabolic profile of lung tissue induced by PPD exposure. A. Pathway classification. B. KEGG enrichment analysis.

pathways (Fig. 11B). Significant decreases in the abundance of *Muribaculaceae* and *Lachnospiraceae*, alongside increases in *Moraxellaceae* and *Staphylococcaceae*, contribute to a marked reduction in SCFAs, exacerbating gut microbiota dysbiosis in mice. Dysregulation of the gut microbiota can lead to mitochondrial damage and dysfunction, triggering oxidative stress responses [61]. Concurrently, the decreased abundance of *Muribaculaceae* leads to reduced levels of reduced glutathione, while increased oxidative glutathione levels exacerbate iron death [62]. Furthermore, the decrease in *Muribaculaceae* abundance, coupled with the increase in *Staphylococcaceae* and *Planococcaceae*, results in alterations in the levels of O-Phosphoethanolamine within the metabolic profile, affecting the glycerophospholipid pathway. These major microbial abundance changes disrupt multiple amino acid metabolic pathways via critical metabolites, ultimately contributing to the onset of pneumonia.

4.7. Current limitations and future research prospect

This study builds on our research team's previously published work. Based on various data indicators, the risk of lung inflammation caused by PPD is significantly higher than that of the same doses of plasticizers or microplastic particles. Therefore, the absence of separate exposure groups for PBD and PS-MPs in this study is a limitation. Additionally, while this research has identified oxidative stress and ferroptosis as key pathways in PPD-induced pneumonia, the exploration of these pathways remains insufficient. The current conclusions regarding the relationship between gut microbiota and lung metabolism are derived solely from the analysis of omics data, and the groupings have certain limitations. Future research will focus on the specific molecular interactions and signaling cascades related to ferroptosis and their direct effects on Th2-mediated responses, with more detailed and in-depth studies. We will also increase the groupings in the omics experiments to obtain more comprehensive omics data, utilizing network analysis and environmental factor association analysis to further elucidate the connections between the two omics. Experiments will be conducted on specific key metabolites and differentially abundant bacterial communities, and the use of specific microbial inhibitors, to identify effective metabolic regulation targets and potential microbial targets.

5. Conclusion

The study reveals the mechanisms by which PPD induces pneumonia in mice from two perspectives. On one hand, after entering the lungs via the systemic circulation, PPD leads to increased levels of ROS, IL-4, TNF-α, and IL-1β in the lungs of mice, while decreasing TFN-γ. This can result in ferroptosis of lung cells and ROS-Th2-dominant pneumonia. On the other hand, exposure to PPD causes changes in the gut microbiota structure of mice, particularly a decrease in probiotics such as *Muribaculaceae* and *Lachnospiraceae*, and an increase in *Moraxellaceae, Staphylococcaceae*, and *Planococcaceae*. These changes are closely associated with alterations in metabolite levels (such as short-chain fatty acids, phospholipids, and multi-amino acids) through the lung-gut axis. The pathways involved include ferroptosis, arachidonic acid metabolism, glycerophospholipid metabolism, oxidative stress, and amino acid metabolism. Furthermore, the study demonstrates that deferoxamine (DFO) can alleviate PPD-induced pneumonia. This research, for the first time, elucidated the communication between lung and gut environments triggered by PPD exposure, shedding light on the molecular mechanisms underlying pneumonia induction and progression due to PPD. This enhances our understanding of PPD toxicology and provides a theoretical foundation for the treatment of this type of pneumonia.

Enviromental implication

Plastic pollution derivatives (PPD) are fragments like microplastics and chemical components such as plasticizers, formed through various environmental processes from discarded plastics. PPD pose greater health risks than the original plastic products, as they can enter the food chain and cause significant harm. This study focuses on polystyrene microplastics (PS-MPs) and dibutyl phthalate (DBP), two common PPD, to explore their combined effects on pneumonia risk. The research enhances our understanding of PPD health impacts and offers a theoretical foundation for mitigating associated health risks.

CRediT authorship contribution statement

Xu Yang: Writing – review & editing, Writing – original draft, Visualization, Validation, Software, Resources, Project administration, Methodology. **Yang Wu:** Writing – review & editing, Validation, Resources. **Qing Feng:** Writing – review & editing, Writing – original draft, Visualization, Software, Methodology, Data curation, Conceptualization. **Surui Lu:** Writing – review & editing, Writing – original draft, Visualization, Software, Resources, Methodology, Formal analysis, Data curation, Conceptualization. **Ping Ma:** Writing – review & editing, Validation, Resources, Project administration, Investigation, Funding acquisition, Conceptualization. **Hai Guo:** Writing – review & editing,

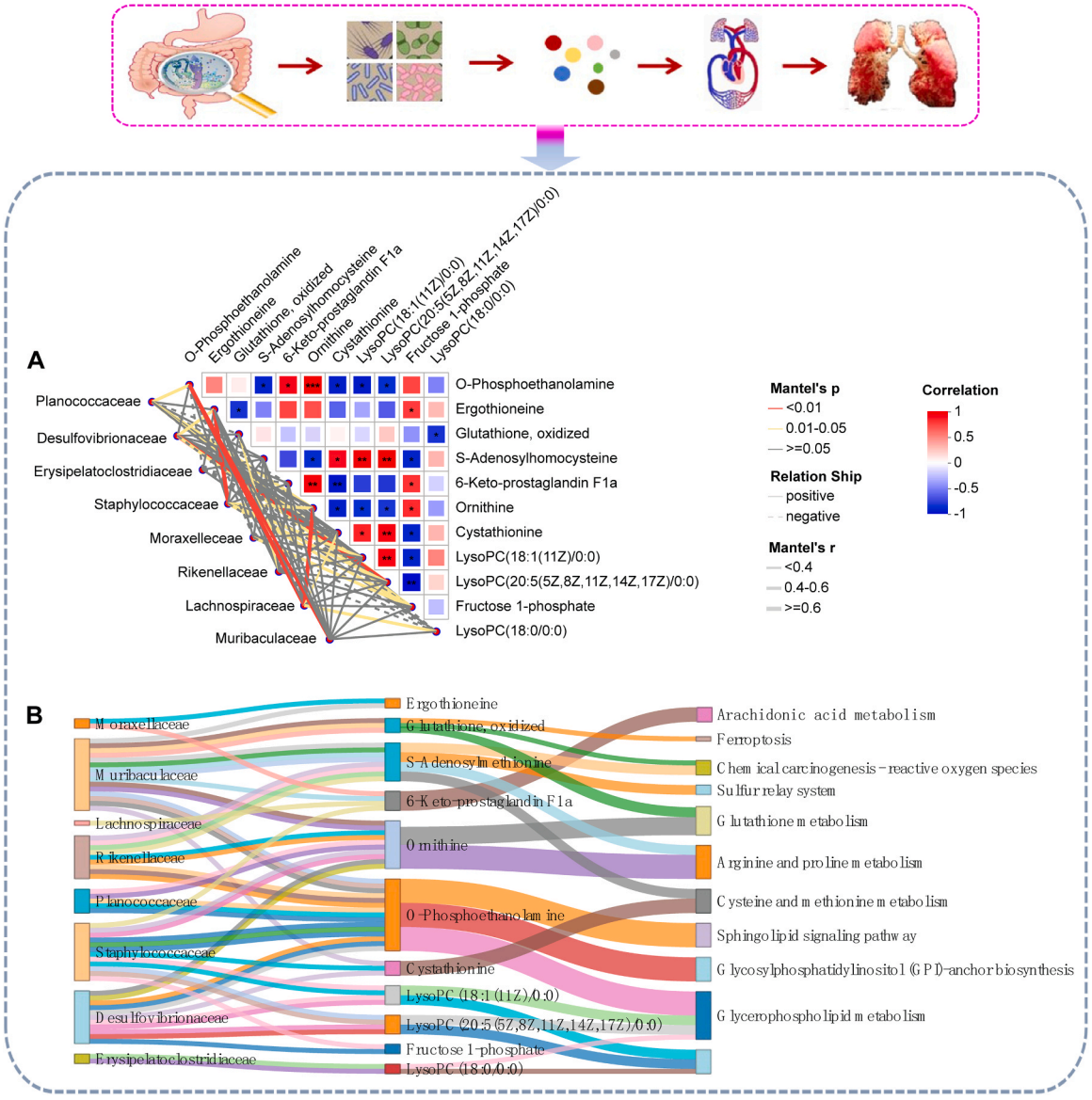

Fig. 11. The association between the microbiome and the metabolome. A: The cascade network from microbiotas, to matabolites, and to pathways in lung. B: Mantel test heatmap: The lines in the figure represent the correlation between communities and environmental factors, while the heatmap shows the correlations between environmental factors. The thickness of the lines indicates the strength of the correlation between communities and environmental factors, plotted using the absolute value of Mantel's r (|R|). The labels "Positive" and "Negative" denote the positive and negative correlations between communities and environmental factors, respectively. Different colors in the heatmap represent positive and negative correlations, with color intensity reflecting the strength of these correlations. Asterisks in the blocks indicate significance: *0.01 < P ≤ 0.05, ** 0.001 < P ≤ 0.01, *** P ≤ 0.001.".

Validation, Resources. **Qizi Chen:** Writing – review & editing, Writing – original draft, Resources. **Biao Yan:** Writing – review & editing, Validation, Resources. **Liqin Su:** Writing – review & editing, Resources, Funding acquisition. **Huaqin Wei:** Writing – original draft, Resources, Methodology, Formal analysis, Data curation. **Xin Zeng:** Writing – review & editing, Writing – original draft, Software, Data curation. **Mingqing Chen:** Writing – review & editing, Validation, Investigation, Funding acquisition.

Declaration of Competing Interest

The authors declare that they have no known competing financial interests or personal relationships that could have appeared to influence the work reported in this paper.

Acknowledgments

This work was supported by the National Natural Science Foundation of China (42177416, 42477452), Key Special Project for Social Development R&D of Xianning City Science and Technology Program (2021SFYF007, 2023SFYF095), and Scientific Research Innovative Team of Hubei University of Science and Technology (2023T08).

Appendix A. Supporting information

Supplementary data associated with this article can be found in the online version at doi:10.1016/j.jhazmat.2024.136326.

Data availability

Data will be made available on request.

References

[1] Kibria, M.G., Masuk, N.I., Safayet, R., Nguyen, H.Q., Mourshed, M., 2023. Plastic Waste: Challenges and Opportunities to Mitigate Pollution and Effective Management. Int J Environ Res 17 (1), 20. https://doi.org/10.1007/s41742-023-00507-z.

[2] MacLeod, M., Arp, H.P.H., Tekman, M.B., Jahnke, A., 2021. The global threat from plastic pollution. Science 373 (6550), 61–65. https://doi.org/10.1126/science.abg5433.

[3] Lin, L., Yuan, B., Liu, H., Ke, Y., Zhang, W., Li, H., et al., 2024. Microplastics emerge as a hotspot for dibutyl phthalate sources in rivers and oceans: Leaching behavior and potential risks. J Hazard Mater 475, 134920. https://doi.org/10.1016/j.jhazmat.2024.134920.

[4] Yan, Y., Zhu, F., Zhu, C., Chen, Z., Liu, S., Wang, C., et al., 2021. Dibutyl phthalate release from polyvinyl chloride microplastics: Influence of plastic properties and environmental factors. Water Res 204, 117597. https://doi.org/10.1016/j.watres.2021.117597.

[5] Zhang, S.Q., Li, P., He, S.W., Xing, S.Y., Cao, Z.H., Zhao, X.L., et al., 2023. Combined effect of microplastic and triphenyltin: Insights from the gut-brain axis. Environ Sci Ecotechnol 16, 100266. https://doi.org/10.1016/j.ese.2023.100266.

[6] Jin, W., Zhang, W., Tang, H., Wang, P., Zhang, Y., Liu, S., et al., 2024. Microplastics exposure causes the senescence of human lung epithelial cells and mouse lungs by inducing ROS signaling. Environ Int 185, 108489. https://doi.org/10.1016/j.envint.2024.108489.

[7] Mei, L.T., Chee, K.Y., Shahrul, B.S.H., 2022. Plastic pollution and sustainable managing of single-use laboratory plastic waste. Sustain Clim Chang 15 (1), 6–16. https://doi.org/10.1089/scc.2021.0050.

[8] eClinicalMedicine, 2023. Plastic pollution and health. EClinicalMedicine 60, 102074. https://doi.org/10.1016/j.eclinm.2023.102074.

[9] Tao, H.Y., Shi, J., Zhang, J., Ge, H., Zhang, M., Li, X.Y., 2024. Developmental toxicity and mechanism of dibutyl phthalate and alternative diisobutyl phthalate in the early life stages of zebrafish (Danio rerio). Aquat Toxicol 272, 106962. https://doi.org/10.1016/j.aquatox.2024.106962.

[10] Nahla, E., Arya, P., Maneesha, P., Chitra, K.C., 2024. Exposure to the plasticizer dibutyl phthalate causes oxidative stress and neurotoxicity in brain tissue. Environ Sci Pollut Res Int 31 (14), 21399–21414. https://doi.org/10.1007/s11356-024-32604-7.

[11] Wang, C., Yao, X.F., Li, X.X., Wang, Q., Wang, J.H., Zhu, L.S., et al., 2023. Effects of dibutyl phthalate on microbial community and the carbon cycle in salinized soil. J Clean Prod 404 (0), 136928–1369218. https://doi.org/10.1016/j.jclepro.2023.136928.

[12] Wang, X., Han, B., Wu, P., Li, S., Lv, Y., Lu, J., et al., 2020. Dibutyl phthalate induces allergic airway inflammation in rats via inhibition of the Nrf2/TSLP/JAK1 pathway. Environ Pollut 267, 115564. https://doi.org/10.1016/j.envpol.2020.115564.

[13] Wang, X., Lv, Z., Han, B., Li, S., Yang, Q., Wu, P., et al., 2021. The aggravation of allergic airway inflammation with dibutyl phthalate involved in Nrf2-mediated activation of the mast cells. Sci Total Environ 789, 148029. https://doi.org/10.1016/j.scitotenv.2021.148029.

[14] Zhao, Z., Zheng, X., Han, Z., Li, Y., He, H., Lin, T., et al., 2024. Polystyrene microplastics enhanced the effect of PFOA on Chlorella sorokiniana: perspective from the cellular and molecular levels. J Hazard Mater 465, 133455. https://doi.org/10.1016/j.jhazmat.2024.133455.

[15] Zhang, Q., Ma, W., Zhu, J., 2023. Combined toxicities of di-butyl phthalate and polyethylene terephthalate to zebrafish embryos. Toxics 11 (5), 469. https://doi.org/10.3390/toxics11050469.

[16] Wang, J., Liu, C., Cao, Q., Li, Y., Chen, L., Qin, Y., et al., 2024. Enhanced biodegradation of microplastic and phthalic acid ester plasticizer: the role of gut microorganisms in black soldier fly larvae. Sci Total Environ 924, 171674. https://doi.org/10.1016/j.scitotenv.2024.171674.

[17] Almaiman, L., Aljomah, A., Bineid, M., Aljeldah, F.M., Aldawsari, F., Liebmann, B., et al., 2021. The occurrence and dietary intake related to the presence of microplastics in drinking water in Saudi Arabia. Environ Monit Assess 193 (7), 390. https://doi.org/10.1007/s10661-021-09132-9.

[18] Han, Q., Gao, X., Wang, S., Wei, Z., Wang, Y., Xu, K., et al., 2023. Co-exposure to polystyrene microplastics and di-(2-ethylhexyl) phthalate aggravates allergic asthma through the TRPA1-p38 MAPK pathway. Toxicol Lett 384, 73–85. https://doi.org/10.1016/j.toxlet.2023.07.013.

[19] Ding, R., Chen, Y., Shi, X., Li, Y., Yu, Y., Sun, Z., et al., 2024. Size-dependent toxicity of polystyrene microplastics on the gastrointestinal tract: Oxidative stress related-DNA damage and potential carcinogenicity. Sci Total Environ 912, 169514. https://doi.org/10.1016/j.scitotenv.2023.169514.

[20] Li, Y., Yan, B., Wu, Y., Peng, Q., Wei, Y., Chen, Y., et al., 2023. Ferroptosis participates in dibutyl phthalate-aggravated allergic asthma in ovalbumin-sensitized mice. Ecotoxicol Environ Saf 256, 114848. https://doi.org/10.1016/j.ecoenv.2023.114848.

[21] Zhang, Y., Yang, Z., Li, X., Song, P., Wang, J., 2022. Effects of diisononyl phthalate exposure on the oxidative stress and gut microorganisms in earthworms (Eisenia fetida). Sci Total Environ 822, 153563. https://doi.org/10.1016/j.scitotenv.2022.153563.

[22] Zhang, L., Yu, Y., Yu, R., 2020. Analysis of metabolites and metabolic pathways in three maize (Zea mays L.) varieties from the same origin using GC-MS. Sci Rep 10 (1), 17990. https://doi.org/10.1038/s41598-020-73041-z.

[23] Schrimpe-Rutledge, A.C., Codreanu, S.G., Sherrod, S.D., McLean, J.A., 2016. Untargeted Metabolomics Strategies-Challenges and Emerging Directions. J Am Soc Mass Spectrom 27 (12), 1897–1905. https://doi.org/10.1007/s13361-016-1469-y.

[24] Claus, S.P., Ellero, S.L., Berger, B., Krause, L., Bruttin, A., Molina, J., et al., 2011. Colonization-induced host-gut microbial metabolic interaction. mBio 2 (2), e00271-10. https://doi.org/10.1128/mBio.00271-10.

[25] Diaz Heijtz, R., Wang, S., Anuar, F., Qian, Y., Björkholm, B., Samuelsson, A., et al., 2011. Normal gut microbiota modulates brain development and behavior. Proc Natl Acad Sci USA 108 (7), 3047–3052. https://doi.org/10.1073/pnas.1010529108.

[26] Tu, P., Xue, J., Niu, H., Tang, Q., Mo, Z., Zheng, X., et al., 2023. Deciphering gut microbiome responses upon microplastic exposure via integrating metagenomics and activity-based metabolomics. Metabolites 13 (4), 530. https://doi.org/10.3390/metabo13040530.

[27] Fiehn, O., 2016. Metabolomics by gas chromatography-mass spectrometry: combined targeted and untargeted profiling, 4.32 Curr Protoc Mol Biol 114 (30.4), 1–30. https://doi.org/10.1002/0471142727.mb3004s114.

[28] Lee-Sarwar, K.A., Lasky-Su, J., Kelly, R.S., Litonjua, A.A., Weiss, S.T., 2020. Gut Microbial-Derived Metabolomics of Asthma. Metabolites 10 (3), 97. https://doi.org/10.3390/metabo10030097.

[29] Yan, M., Xu, G., 2018. Current and future perspectives of functional metabolomics in disease studies-A review. Anal Chim Acta 1037, 41–54. https://doi.org/10.1016/j.aca.2018.04.006.

[30] Song, W., Yue, Y., Zhang, Q., 2023. Imbalance of gut microbiota is involved in the development of chronic obstructive pulmonary disease: A review. Biomed Pharmacother 165, 115150. https://doi.org/10.1016/j.biopha.2023.115150.

[31] Almamoun, R., Pierozan, P., Manoharan, L., Karlsson, O., 2023. Altered gut microbiota community structure and correlated immune system changes in dibutyl phthalate exposed mice. Ecotoxicol Environ Saf 262, 115321. https://doi.org/10.1016/j.ecoenv.2023.115321.

[32] Gomaa, E.Z., 2020. Human gut microbiota/microbiome in health and diseases: a review. Antonie Van Leeuwenhoek 113 (12), 2019–2040. https://doi.org/10.1007/s10482-020-01474-7.

[33] Park, S.Y., An, K.S., Lee, B., Kang, J.H., Jung, H.J., Kim, M.W., et al., 2021. Establishment of particulate matter-induced lung injury model in mouse. Lab Anim Res 37 (1), 20. https://doi.org/10.1186/s42826-021-00097-x.

[34] Wei, H., Lu, S., Chen, M., Yao, R., Yan, B., Li, Q., et al., 2024. Mechanisms of exacerbation of Th2-mediated eosinophilic allergic asthma induced by plastic pollution derivatives (PPD): a molecular toxicological study involving lung cell ferroptosis and metabolomics. The (Advance online publication). Sci Total Environ 946, 174482. https://doi.org/10.1016/j.scitotenv.2024.174482.

[35] Shi, C., Han, X., Guo, W., Wu, Q., Yang, X., Wang, Y., et al., 2022. Disturbed Gut-Liver axis indicating oral exposure to polystyrene microplastic potentially increases the risk of insulin resistance. Environ Int 164, 107273. https://doi.org/10.1016/j.envint.2022.107273.

[36] Hernandez, L.M., Xu, E.G., Larsson, H.C.E., Tahara, R., Maisuria, V.B., Tufenkji, N., 2019. Plastic teabags release billions of microparticles and nanoparticles into tea. Environ Sci Technol 53 (21), 12300–12310. https://doi.org/10.1021/acs.est.9b02540.

[37] Pierozan, P., Källsten, L., Theodoropoulou, E., Almamoun, R., Karlsson, O., 2023. Persistent immunosuppressive effects of dibutyl phthalate exposure in adult male mice. Sci Total Environ 878, 162741. https://doi.org/10.1016/j.scitotenv.2023.162741.

[38] Fernández, P.M., Viñarta, S.C., Bernal, A.R., Cruz, E.L., Figueroa, L.I.C., 2018. Bioremediation strategies for chromium removal: current research, scale-up approach and future perspectives. Chemosphere 208, 139–148. https://doi.org/10.1016/j.chemosphere.2018.05.166.

[39] Yuan, J., Li, J., Du, S., Wen, Y., Wang, Y., Lang, Y.F., et al., 2024. Revealing the lethal effects of Pasteurella multocida toxin on multiple organ systems. Front Microbiol 15, 1459124. https://doi.org/10.3389/fmicb.2024.1459124.

[40] Zhou, S., Han, M., Ren, Y., Yang, X., Duan, L., Zeng, Y., et al., 2020. Dibutyl phthalate aggravated asthma-like symptoms through oxidative stress and increasing calcitonin gene-related peptide release. Ecotoxicol Environ Saf 199, 110740. https://doi.org/10.1016/j.ecoenv.2020.110740.

[41] Chandrasekaran, A., Idelchik, M.D.P.S., Melendez, J.A., 2017. Redox control of senescence and age-related disease. Redox Biol 11, 91–102. https://doi.org/10.1016/j.redox.2016.11.005.

[42] Roan, F., Obata-Ninomiya, K., Ziegler, S.F., 2019. Epithelial cell-derived cytokines: more than just signaling the alarm. J Clin Invest 129 (4), 1441–1451. https://doi.org/10.1172/JCI124606.

[43] Ren, J.X., Sun, X., Yan, X.L., Guo, Z.N., Yang, Y., 2020. Ferroptosis in neurological diseases. Front Cell Neurosci 14, 218. https://doi.org/10.3389/fncel.2020.00218.

[44] Wang, S., Xia, P., Huang, G., Zhu, P., Liu, J., Ye, B., et al., 2016. FoxO1-mediated autophagy is required for NK cell development and innate immunity. Nat Commun 7, 11023. https://doi.org/10.1038/ncomms11023.

[45] Ferrini, M., Carvalho, S., Cho, Y.H., Postma, B., Miranda Marques, L., Pinkerton, K., et al., 2017. Prenatal tobacco smoke exposure predisposes offspring mice to exacerbated allergic airway inflammation associated with altered innate effector function. Part Fibre Toxicol 14 (1), 30. https://doi.org/10.1186/s12989-017-0212-6.

[46] Shrestha P.N., Mackenzie, C.A., Licskai, C., Kim, R.B., Vliagoftis, H., Cameron, L., 2022. The CRTh2 polymorphism rs533116 G > A associates with asthma severity in older females. Front. Med (Lausanne). 9, 970495. https://doi.org/10.3389/fmed.2022.970495.

[47] Peng, Q., Wu, Y., Li, Y., Lu, C., Yao, R., Hu, S., et al., 2024. The IL-31/TRPV1 pathway mediates allergic asthma exacerbated by DINP dermal exposure in OVA-

sensitized Balb/c mice. Sci Total Environ 912, 169613. https://doi.org/10.1016/j.scitotenv.2023.169613.
[48] Xie, X., Li, Y., Yan, B., Peng, Q., Yao, R., Deng, Q., et al., 2024. Mediation of the JNC/ILC2 pathway in DBP-exacerbated allergic asthma: a molecular toxicological study on neuroimmune positive feedback mechanism. J Hazard Mater 465, 133360. https://doi.org/10.1016/j.jhazmat.2023.133360.
[49] Choi, Y., Le Pham, D., Lee, D.H., Lee, S.H., Kim, S.H., Park, H.S., 2018. Biological function of eosinophil extracellular traps in patients with severe eosinophilic asthma. Exp Mol Med 50 (8), 1–8. https://doi.org/10.1038/s12276-018-0136-8.
[50] Jang, Y.O., Lee, S.H., Choi, J.J., Kim, D.H., Choi, J.M., Kang, M.J., et al., 2020. Fecal microbial transplantation and a high fiber diet attenuates emphysema development by suppressing inflammation and apoptosis. Exp Mol Med 52 (7), 1128–1139. https://doi.org/10.1038/s12276-020-0469-y.
[51] Sun, J., Gou, Y., Liu, J., Chen, H., Kan, J., Qian, C., et al., 2020. Anti-inflammatory activity of a water-soluble polysaccharide from the roots of purple sweet potato. Rsc Adv 10 (65), 39673–39686. https://doi.org/10.1039/d0ra07551e.
[52] Guo, M., Li, Z., 2019. Polysaccharides isolated from Nostoc commune Vaucher inhibit colitis-associated colon tumorigenesis in mice and modulate gut microbiota. Food Funct 10 (10), 6873–6881. https://doi.org/10.1039/c9fo00296k.
[53] Gupta, N., Abd El-Gawaad, N.S., Osman Abdallah, S.A., Al-Dossari, M., 2024. Possible modulating functions of probiotic Lactiplantibacillus plantarum in particulate matter-associated pulmonary inflammation. Front Cell Infect Microbiol 13, 1290914. https://doi.org/10.3389/fcimb.2023.1290914.
[54] Naito, Y., Kashiwagi, K., Takagi, T., Andoh, A., Inoue, R., 2018. Intestinal Dysbiosis Secondary to Proton-Pump Inhibitor Use. Digestion 97 (2), 195–204. https://doi.org/10.1159/000481813.
[55] Zhao, D., Gao, Y., Chen, Y., Zhang, Y., Deng, Y., Niu, S., et al., 2024. L-Citrulline ameliorates iron metabolism and mitochondrial quality control via activating AMPK pathway in intestine and improves microbiota in mice with iron overload. Mol Nutr Food Res 68 (6), e2300723.
[56] Ni, K., Che, B., Gu, R., Wang, C., Xu, H., Li, H., et al., 2024. BitterDB database analysis plus cell stiffness screening identify flufenamic acid as the most potent TAS2R14-based relaxant of airway smooth muscle cells for therapeutic bronchodilation. Theranostics 14 (4), 1744–1763. https://doi.org/10.7150/thno.92492.
[57] Zhang, H., Zhang, C., Hua, W., Chen, J., 2024. Saying no to SARS-CoV-2: the potential of nitric oxide in the treatment of COVID-19 pneumonia. Med Gas Res 14 (2), 39–47. https://doi.org/10.4103/2045-9912.385414.
[58] Tian, S., Liu, W., Liu, B., Ye, F., Xu, Z., Wan, Q., et al., 2024. Mechanistic study of C5F10O-induced lung toxicity in rats: An eco-friendly insulating gas alternative to SF6. Sci Total Environ 916, 170271. https://doi.org/10.1016/j.scitotenv.2024.170271.
[59] Dai, S., Wang, Z., Cai, M., Guo, T., Mao, S., Yang, Y.A., 2024. multi-omics investigation of the lung injury induced by PM2.5 at environmental levels via the lung-gut axis. Sci Total Environ 926, 172027. https://doi.org/10.1016/j.scitotenv.2024.172027.
[60] Xu, L., Zhang, L., Xiang, Y., Zhang, X., 2024. Knockdown of lncRNA NEAT1 suppresses streptococcus pneumoniae-induced ferroptosis in alveolar epithelial cells by regulating the Nrf2-GPX4 pathway. Toxicon 243, 107705. https://doi.org/10.1016/j.toxicon.2024.107705.
[61] He, J., Liu, R., Zheng, W., Guo, H., Yang, Y., Zhao, R., et al., 2021. High ambient temperature exposure during late gestation disrupts glycolipid metabolism and hepatic mitochondrial function tightly related to gut microbial dysbiosis in pregnant mice. Micro Biotechnol 14 (5), 2116–2129. https://doi.org/10.1111/1751-7915.13893.
[62] Chen, Y.L., Wu, J.M., Chen, K.Y., Wu, M.H., Yang, P.J., Lee, P.C., et al., 2024. Intravenous calcitriol administration improves the liver redox status and attenuates ferroptosis in mice with high-fat diet-induced obesity complicated with sepsis (Advance online publication). Biomed Pharmacother 177, 116926. https://doi.org/10.1016/j.biopha.2024.116926.